THE JOURNAL OF BIOLOGICAL CHEMISTRY VOL. 283, NO. 50, pp. 34923–34934, December 50, 2008

Assembly of High Order Gα_q-Effector Complexes with RGS Proteins*[S]

Received for publication, July 30, 2008, and in revised form, September 25, 2008 Published, JBC Papers in Press, October 20, 2008, DOI 10.1074/jbc.M805860200

Aruna Shankaranarayanan[‡§], David M. Thal[‡¶], Valerie M. Tesmer[‡], David L. Roman[‖1], Richard R. Neubig[‖], Tohru Kozasa[**], and John J. G. Tesmer[‡¶‖2]

From the [‡]Life Sciences Institute, University of Michigan, Ann Arbor, Michigan 48109-2216, the [§]Institute for Cellular and Molecular Biology, University of Texas, Austin, Texas 78712, the [¶]Chemical Biology Program, University of Michigan, Ann Arbor, Michigan 48109-1055, the [‖]Department of Pharmacology, University of Michigan, Ann Arbor, Michigan 48109-5632, and the [**]Department of Pharmacology, University of Illinois, Chicago, Illinois 60612

Transmembrane signaling through Gα_q-coupled receptors is linked to physiological processes such as cardiovascular development and smooth muscle function. Recent crystallographic studies have shown how Gα_q interacts with two activation-dependent targets, p63RhoGEF and G protein-coupled receptor kinase 2 (GRK2). These proteins bind to the effector-binding site of Gα_q in a manner that does not appear to physically overlap with the site on Gα_q bound by regulator of G-protein signaling (RGS) proteins, which function as GTPase-activating proteins (GAPs). Herein we confirm the formation of RGS-Gα_q-GRK2/p63RhoGEF ternary complexes using flow cytometry protein interaction and GAP assays. RGS2 and, to a lesser extent, RGS4 are negative allosteric modulators of Gα_q binding to either p63RhoGEF or GRK2. Conversely, GRK2 enhances the GAP activity of RGS4 but has little effect on that of RGS2. Similar but smaller magnitude responses are induced by p63RhoGEF. The fact that GRK2 and p63RhoGEF respond similarly to these RGS proteins supports the hypothesis that GRK2 is a *bona fide* Gα_q effector. The results also suggest that signal transduction pathways initiated by GRK2, such as the phosphorylation of G protein-coupled receptors, and by p63RhoGEF, such as the activation of gene transcription, can be regulated by RGS proteins via both allosteric and GAP mechanisms.

Heterotrimeric GTP-binding (G) proteins (G$\alpha\beta\gamma$) relay the extracellular signals received by G protein-coupled receptors (GPCRs)[3] to effector enzymes and channels in the cell (1). Activated GPCRs catalyze nucleotide exchange on Gα subunits, thereby converting the inactive (GDP-bound) G$\alpha\beta\gamma$ heterotrimer into activated Gα·GTP and G$\beta\gamma$ subunits. These subunits then interact with downstream effectors to elicit intracellular responses (2). Duration of signaling is limited by the rate of GTP hydrolysis on the Gα subunit. After returning to the GDP-bound state, Gα reforms the inactive G$\alpha\beta\gamma$ heterotrimer, which can then undergo additional rounds of receptor-mediated activation. For some families of Gα subunits, the rate of GTP hydrolysis can be accelerated by direct interactions with effectors (3, 4) or regulator of G protein signaling (RGS) proteins (5, 6). Although RGS proteins are generally thought of as inhibitors of heterotrimeric G protein signaling mediated by the Gα_i and G$\alpha_{q/11}$ families, they may also serve to spatially focus the signals being propagated (7) or to regulate the steady-state flux through a specific signaling cascade (8).

Comparison of the crystal structures of the Gα_i-RGS4 (9) and Gα_s-adenylyl cyclase (10) complexes revealed that RGS proteins and effectors interact with discrete footprints on the surface of Gα and have the potential to bind simultaneously (11, 12). Direct experimental support for an RGS-Gα-effector ternary complex came from analysis of the interactions of transducin (Gα_t) with RGS proteins and the γ subunit of cGMP phosphodiesterase (PDEγ). Both PDEγ (13) and RGS9 (14) are required for physiological rates of GTP hydrolysis on Gα_t. Although PDEγ has no GAP activity on its own, it can stimulate RGS9-mediated GAP activity by up to ~3-fold (14). Mutagenesis studies (15), biophysical measurements (16), and ultimately the crystal structure of the RGS9-G$\alpha_{t/i1}$-PDEγ ternary complex (17) were all consistent with a model of allosteric modulation between the effector and RGS binding sites of Gα_t, with little or no direct functional interaction between PDEγ and RGS9. It has been proposed that this PDEγ-regulated GAP activity prevents a "short circuit" of the phototransduction cascade via premature hydrolysis of Gα_t·GTP before effectors can functionally interact with the G protein (18). Conversely, PDEγ inhibits the GAP activity of other RGS proteins (RGS4, GAIP, and RGS16/RGSr) most likely through a negative allosteric mechanism (18–20). It is not known whether analogous ternary complexes

* This work was supported, in whole or in part, by National Institutes of Health Grants HL086865 and HL071818 (to J. J. G. T.), GM61454 (to T. K.), DA23252 (to R. R. N.), and GM076821 (to D. L. R.). This work was also supported by an American Heart Association Greater Midwest Affiliate grant-in-aid (to T. K.) and a predoctoral fellowship from the Midwest Affiliate of the American Heart Association (to A. S.). The costs of publication of this article were defrayed in part by the payment of page charges. This article must therefore be hereby marked "*advertisement*" in accordance with 18 U.S.C. Section 1734 solely to indicate this fact.

[S] The on-line version of this article (available at http://www.jbc.org) contains supplemental Figs. S1 and S2.

[1] Current address: University of Iowa, College of Pharmacy, Iowa City, IA 52242-1112.

[2] To whom correspondence should be addressed: 210 Washtenaw Ave, Ann Arbor, MI 48109-2216. Tel.: 734-615-9544; Fax: 734-763-6492; E-mail: johntesmer@umich.edu.

[3] The abbreviations used are: GPCR, G protein-coupled receptor; RGS, regulator of G-protein signaling; PDE, phosphodiesterase; FCPIA, flow cytometry protein interaction assay; AF, Alexa Fluor; MFI, median fluorescence intensity; GAP, GTPase-activating protein; GEF, guanine nucleotide exchange factor; GRK2, G protein-coupled receptor kinase 2; DTT, dithiothreitol; CHAPS, 3-[(3-cholamidopropyl)dimethylammonio]-1-propanesulfonic acid; GTPγS, guanosine 5′-3-*O*-(thio)triphosphate.

are formed by other members of the $G\alpha_i$ family or by subunits from the $G\alpha_q$ family or if there are other effector/RGS combinations that are synergistic with respect to GAP activity on $G\alpha$.

The $G_{q/11}$ family of G proteins is involved in an array of cellular processes that include platelet activation, cardiovascular development, and regulation of memory, appetite, motor coordination, and sleep (21, 22). They are also strongly implicated in pathophysiological processes such as the development of cardiac hypertrophy (23) and high blood pressure (24). Although the canonical effector of $G\alpha_q$ is phospholipase Cβ (PLCβ) (25), recent structural, biochemical, and whole animal studies have confirmed that the Trio family of RhoA guanine nucleotide exchange factors (RhoGEFs), namely Trio, Duet, and p63RhoGEF, are also direct targets of $G\alpha_q$ (26–29), thereby linking $G\alpha_q$ to RhoA-mediated processes such as cell migration, proliferation, and contraction. Another putative effector target of $G\alpha_q$ is G protein-coupled receptor kinase 2 (GRK2) (30). GRK2 phosphorylates activated heptahelical receptors, which are then bound by arrestin and targeted for endocytosis (31). Furthermore, through a process known as phosphorylation-independent desensitization (32–34), GRK2 is thought to sequester activated $G\alpha_q$ from PLCβ using its amino-terminal RGS homology (RH) domain (35, 36). The crystal structure of the $G\alpha_q$-GRK2-G$\beta\gamma$ complex revealed that GRK2 binds to the effector-binding site of $G\alpha_q$ (36), raising the possibility that GRK2 is in fact an effector that can initiate its own signaling cascades in response to the activation of $G\alpha_q$. Although one obvious pathway is simply the phosphorylation of activated GPCRs, GRK2 has also recently been reported to phosphorylate insulin receptor substrate-1 (37), p38 MAPK (38), and ezrin (39) in response to GPCR activation.

The rate of GTP hydrolysis by $G\alpha_q$ can be accelerated by many different RGS proteins (22), but two of the best characterized are RGS2 and RGS4, which are both members of the RGS B/R4 subfamily (40, 41). These are relatively simple RGS proteins that consist of an amino-terminal membrane-targeting domain followed by a conserved ~120-amino acid catalytic RGS domain that interacts with the three switch regions of the Gα subunit (9). In cells, RGS4 inhibits both $G\alpha_i$- and $G\alpha_q$-mediated signaling (42), whereas RGS2 is selective for $G\alpha_q$ (43–48). Both proteins have been reported to serve as effector antagonists because they can inhibit PLCβ signaling by either GTPase-deficient Gα subunits or Gα subunits loaded with nonhydrolyzable GTP analogs (43, 49, 50).

In this study we have used biophysical and kinetic studies to demonstrate the formation of ternary complexes of $G\alpha_q$, RGS proteins, and effectors. We also show that RGS2 and RGS4 are negative allosteric modulators of proteins that bind to the effector-binding site of $G\alpha_q$, providing the molecular basis for their reported roles as effector antagonists. Conversely, GRK2 and p63RhoGEF are shown to be allosteric modulators of RGS GAP activity. GRK2 is able to stimulate RGS4 GAP activity on $G\alpha_q$ to a similar extent as PDEγ does for RGS9 GAP activity on $G\alpha_t$. These data provide important insights into the regulation of GRK2 and p63RhoGEF by both $G\alpha_q$ and RGS proteins *in vivo*.

EXPERIMENTAL PROCEDURES

Purification of RGS2 and ΔN-RGS2—cDNA encoding human RGS2 and an amino-terminal deletion of RGS2 (ΔN-RGS2, spanning amino acid residues 72–211) were cloned into the pMALc2H_{10}T vector (51) using the BamHI and SalI restriction sites. The proteins were expressed as tobacco etch virus protease-cleavable maltose-binding protein fusion proteins. All purification steps were performed at 4 °C or on ice. Induced Rosetta (DE3) pLys cell pellets were resuspended in lysis buffer (20 mM HEPES, pH 8.0, 500 mM NaCl, 10 mM β-mercaptoethanol) plus 1 μM leupeptin, 1 mM lima bean trypsin inhibitor, and 0.1 mM phenylmethylsulfonyl fluoride. Cells were lysed with an Avestin C3 homogenizer, ultracentrifuged at 40,000 rpm for 1 h using a Beckman Type Ti 45 rotor, and then loaded on a nickel-nitrilotriacetic acid column pre-equilibrated with lysis buffer. Maltose-binding protein-RGS2 was eluted with lysis buffer containing 150 mM imidazole, pH 8.0, and then treated with 2% (w/w) tobacco etch virus protease and dialyzed against lysis buffer overnight. The dialyzed protein was passed back over a nickel-nitrilotriacetic acid column equilibrated with lysis buffer to remove His-tagged maltose-binding protein and uncut fusion protein. RGS2 was then concentrated in a 30-kDa Centriprep (Millipore) and further purified using two tandem Superdex S200 columns (GE Healthcare) equilibrated with 20 mM HEPES, pH 8.0, 500 mM NaCl and 5 mM DTT. Some of the RGS2 used in these studies was produced from a His_{10}-RGS2 vector (a gift from Scott Heximer, University of Toronto). Purification of His_{10}-RGS2 was as previously described (52).

Purification of Other Proteins—A $G\alpha_{i/q}$ chimera, in which the amino-terminal helix of $G\alpha_q$ is replaced with that of $G\alpha_i$ (36), a fragment of human p63RhoGEF spanning residues 149–502 (henceforth referred to as p63RhoGEF), GRK2, and RGS4 were purified as previously described (9, 27, 53). A construct expressing a fragment of RGS4 analogous to ΔN-RGS2 (ΔN-RGS4, spanning amino acid residues 51–205) was created in pMALc2H_{10}T using the EcoRI and HindIII restriction sites. The overexpressed protein was purified essentially as described for RGS2 except using 100 instead of 500 mM NaCl. Point mutants RGS2-N149D, RGS4-N128G, GRK2-D110A, and p63RhoGEF-F471E were purified as described for their respective wild-type proteins. Purification of $G\alpha_{i/q}$R183C was performed as described for $G\alpha_{i/q}$ with the following modifications. The nickel-column eluate was supplemented with 10% glycerol, and proteins were dialyzed overnight against dialysis buffer (20 mM HEPES, pH 8.0, 100 mM NaCl, 2 mM DTT, 1 mM $MgCl_2$, 50 μM GDP, and 10% glycerol) and concentrated to ~8 mg/ml. $G\alpha_{i/q}$R183C was purified on two tandem S200 gel filtration columns pre-equilibrated with 20 mM HEPES, pH 8.0, 200 mM NaCl, 5 mM DTT, 5 mM $MgCl_2$, 50 μM GDP, and 5% glycerol. $G\alpha_{i/q}$R183C was purified to greater than 90% homogeneity as judged by SDS-PAGE and was concentrated to ~3 mg/ml and then frozen in tubes on liquid nitrogen in volumes of 5 μl.

Flow Cytometry Protein Interaction Assay—Equilibrium binding of either RGS2, RGS4, GRK2, or p63RhoGEF to $G\alpha_{i/q}$ was measured by flow cytometry protein interaction assay (FCPIA). RGS2 and GRK2 were fluorescently labeled either with amine reactive Alexa Fluor (AF) 532 carboxylic acid suc-

cinimidyl ester or with the thiol-reactive AF 532 C_5-maleimide (Invitrogen). Both probes gave similar results in binding assays. RGS4 and p63RhoGEF were labeled only with the thiol-reactive fluorophore. $G\alpha_{i/q}$ was initially biotinylated using biotinamidohexanoic acid *N*-hydroxysuccinimide ester (Sigma) in the form of a $G\alpha_{i/q}\beta\gamma$ heterotrimer, as previously described (27). $G\alpha_{i/q}$ was later biotinylated directly as a monomer because it behaved similarly in binding assays and had the advantage of not requiring separation from $G\beta\gamma$. Biotinylated $G\alpha_{i/q}$ (b-$G\alpha_{i/q}$, 5 nM) was linked to *x*Map LumAvidin microspheres (Luminex) and washed 3 times with 20 mM HEPES, pH 8.0, 100 mM NaCl, 5 mM $MgCl_2$, 0.1% lubrol, 2 mM DTT, 1% bovine serum albumin, 50 μM GDP plus other additions as indicated. The indicated concentrations of AF 532-labeled protein were then added to bead-bound b-$G\alpha_{i/q}$ and then allowed to equilibrate for at least 30 min before being processed on a Luminex 96-well plate bead analyzer. For competition studies, unlabeled proteins were added at the concentrations indicated. Longer incubation times (*e.g.* overnight) did not alter the results, indicating that equilibrium was attained under our assay conditions. The association of AF-labeled protein with beads is reported as the median fluorescence intensity (MFI) for each sample. Each data point was typically measured in duplicate.

Direct binding and competition data were fit by nonlinear regression either to one-site binding equations or to an allosteric model using GraphPad Prism (Version 5.0a). Allosteric modulation of AF-GRK2 binding to $G\alpha_{i/q}$ by RGS proteins was fit using Equations 1 and 2,

$$Y = Y_0 + NS \times [\text{GRK2}] + \frac{[\text{GRK2}] \times B_{max}}{[\text{GRK2}] + K_d'} \qquad \text{(Eq. 1)}$$

where Y is the total fluorescence measured, Y_0 is the background fluorescence, NS is the linear increase in fluorescence due to nonspecific binding of AF-GRK2 to beads, and B_{max} is the maximum fluorescence change due to specific binding. For all but one of the RGS2 dose-response curves (Fig. 5*B*), Y_0 and NS were directly measured and subtracted from the data to obtain specific binding. For these corrected sets, Y_0 and NS were fixed with values of 0. K_d' is the apparent dissociation constant for AF-GRK2,

$$K_d' = K_d \times \frac{(K_A + [\text{A}])}{(K_A + [\text{A}]/\alpha)} \qquad \text{(Eq. 2)}$$

where K_d is the dissociation constant of AF-GRK2 in the absence of allosteric modulation, K_A is the dissociation constant of allosteric modulator A (*i.e.* RGS2 or RGS4) in the absence of AF-GRK2, and α is the cooperativity factor (54). An α value greater than 1 corresponds to negative allostery. K_d, K_A, and α were fit globally from 2–5 separate series of binding saturation curves with automatic outlier rejection as implemented by GraphPad Prism. The dose-response curves were also analyzed using a competitive model wherein the $[\text{A}]/\alpha$ term in Equation 2 was deleted. Model comparisons used the F test as implemented by GraphPad Prism.

Dissociation Rate of GRK2—To determine k_{off} for GRK2 from b-$G\alpha_{i/q}$, 10 nM AF-GRK2 was incubated with bead bound b-$G\alpha_{i/q}$ for 1 or 24 h at 4 °C. Plates were then allowed to equilibrate at room temperature for 30 min, and the dissociation of AF-GRK2 was initiated by adding either unlabeled GRK2 (final concentration 1 μM), GRK2 plus RGS2 (both 1 μM final), or GRK2 plus RGS4 (both 1 μM final). The loss of fluorescence was measured by FCPIA at the indicated time points. Data were fit to a one-phase exponential decay model.

Purification of an RGS4-Gα$_{i/q}$-p63RhoGEF-RhoA Complex—$G\alpha_{i/q}$ and a 1.25 M excess of p63RhoGEF and a 2 M excess of RGS4 were incubated on ice for 30 min in the presence of 20 μM $AlCl_3$ and 10 mM NaF. Total protein concentration was greater than 5 mg/ml. RGS4-$G\alpha_{i/q}$-p63RhoGEF complexes thus formed were gel-filtered through a 2-ml desalting spin column (Zeba^{TM}) to remove excess GDP. RhoA was incubated with 10 mM EDTA on ice for 30 min, and buffer was exchanged with a 0.5-ml spin column to form GDP-free RhoA. The RGS4-$G\alpha_{i/q}$-p63RhoGEF complex was then incubated with 1.5 M excess of GDP-free RhoA on ice for 15 min and then resolved on two tandem Superdex 200 10/300 gel filtration columns pre-equilibrated with 20 mM HEPES, pH 8.0, 50 mM NaCl, 1 mM DTT, 1 μM EDTA, 20 μM $AlCl_3$, and 10 mM NaF.

RGS Protein Pulldown Assays—Mutations in $G\alpha_q$ were generated in mouse $G\alpha_q$ cDNA in pCMV5, and the mutants were expressed in HEK293 cells as previously described (36). RGS2/RGS4 was biotinylated by incubating with equimolar amounts of biotinamidohexanoyl-6-amino-hexanoic acid *N*-hydroxysuccinimide ester (Sigma) on ice for 1 h and then filtering the sample through a 0.5-ml spin column (Zeba^{TM}). $G\alpha_q$ (wild type or the indicated mutant) cell lysates (100 μl) were incubated with 1 μg of biotinylated RGS2/RGS4 and streptavidin beads (Invitrogen) for 3 h at 4 °C in the presence or absence of 30 μM $AlCl_3$, 10 mM NaF. The beads were then washed 3 times with 500 μl of the lysis buffer (±30 μM $AlCl_3$ and 10 mM NaF as appropriate) and then treated with 5 μl of 4× SDS-PAGE loading buffer. $G\alpha_q$ was detected by Western analysis.

GAP Assays—GTPase activation assays were conducted as previously described (55). $G\alpha_{i/q}$R183C (final concentration 1–3 μM) was incubated in a 120-μl GTP mixture (6.25 μM [γ-^{32}P]GTP (30–100 cpm/fmol), 50 mM HEPES, pH 7.4, 1 mM EDTA, 1 mM DTT, 0.9 mM $MgSO_4$, 5.5 mM CHAPS, 0.1 mg/ml bovine serum albumin, 5% glycerol, and 37.5 μM $(NH_4)_2SO_4$) for ~3 h at 20 °C. [γ-^{32}P]GTP-bound $G\alpha_{i/q}$R183C was purified from unbound nucleotide at 4 °C using a 0.5-ml spin column (Zeba^{TM}). A sample of this protein was reserved for liquid scintillation counting to calculate specific activity. GTP hydrolysis was performed in an assay buffer containing 20 mM HEPES, pH 7.4, 80 mM NaCl, 1 mM EDTA, 1 mM DTT, 0.9 mM $MgSO_4$, 1 mM GTP, 0.20% (w/v) cholate, and 10 μg/ml bovine serum albumin. The reaction was initiated by the addition of 30 μl of the [γ-^{32}P]GTP-loaded $G\alpha_{i/q}$R183C to 270 μl of assay buffer at 20 °C either alone or in the presence of additional proteins as indicated. The reaction was terminated at each time point by adding 50 μl of the reaction mix to 750 μl of quench buffer (5% activated charcoal in 50 mM NaH_2PO_4, pH 2) on ice. The radioactivity remaining in the supernatant was quantified by liquid scintillation counting of 300 μl of the supernatant. In each assay typically ~5 nM $G\alpha_{i/q}$R183C was estimated as being loaded with [γ-^{32}P]GTP.

Nucleotide Exchange Assay—Nucleotide exchange on RhoA was measured as previously described (27) except that the reaction mix (2 μM RhoA, 200 nM p63RhoGEF, 400 nM $G\alpha_{i/q}$) and the indicated concentrations of RGS proteins were first equilibrated for 2 h at 4 °C before the addition of 1 μM BODIPY FL GTPγS (Invitrogen).

RESULTS

Crystallographic studies demonstrated that GRK2 and p63RhoGEF both engage $G\alpha_q$ in a manner that would appear to allow the binding of the RGS domain of either RGS4 (9) or RGS2 (56) to $G\alpha_q$ without steric overlap (Fig. 1, *A* and *B*). Models of these RGS-$G\alpha_{i/q}$-effector complexes, thus, resemble the structure of the PDEγ-$G\alpha_{t/i1}$-RGS9 complex (Fig. 1*C*). The positions of the modeled RGS box domains in these complexes are also consistent with the predicted orientation of these complexes at the cell surface in that the membrane binding elements of the RGS proteins are juxtaposed with the phospholipid bilayer. We, therefore, initiated *in vitro* experiments to confirm the formation of these complexes and to better understand the roles of RGS proteins in modulating the interactions of $G\alpha_q$ with GRK2 and p63RhoGEF.

To observe the formation of ternary RGS complexes *in vitro*, we chose to use the FCPIA, wherein a protein receptor is biotinylated and bound to streptavidin-coated beads and the equilibrium binding of a fluorescently labeled ligand is quantitatively assessed by measuring bead-bound fluorescence in a flow cytometer (57, 58). We first measured the direct association of AF 532-labeled GRK2 (AF-GRK2), AF-p63RhoGEF, AF-RGS2, and AF-RGS4 with a biotinylated chimera of $G\alpha_q$·GDP (b-$G\alpha_{i/q}$) activated with AlF_4^- (Fig. 2*A*). Nonspecific binding was determined from the increase in fluorescence using the deactivated, GDP-bound chimera. The $G\alpha_{i/q}$ chimera was used for these experiments because the protein can be expressed at much higher yields in insect cells than wild type (36, 59) and has been used in crystallographic analysis of the $G\alpha_{i/q}$-p63RhoGEF and $G\alpha_{i/q}$-GRK2 complexes (Fig. 1, *A* and *B*). The amino terminus of $G\alpha_q$ is not expected to directly interact with these effectors, and the binding of GRK2 to a different chimera of $G\alpha_q$ that included the native amino terminus of $G\alpha_q$ yielded similar dissociation constants as with $G\alpha_{i/q}$ (data not shown). The p63RhoGEF construct used in this study spans residues 149–502 of the full-length protein and is the minimal fragment required for high affinity $G\alpha_{i/q}$ binding and activation *in vitro* and for full $G\alpha_q$-mediated activation of RhoA *in vivo* (27). AF-GRK2, AF-p63RhoGEF, AF-RGS2, and AF-RGS4 bound to $G\alpha_{i/q}$ with dissociation constants of 3, 80, 3, and 5 nM, respectively (Table 1, Fig. 2, *B*–*E*). The MFI at which these binding curves saturate likely varies due to different efficiencies of fluorescent labeling for each protein.

Because an AF-labeled protein may not bind with the same affinity as the unmodified protein, we used homologous competition experiments (Fig. 3*A*) to determine the equilibrium dissociation constants for GRK2, p63RhoGEF, RGS2, and RGS4. In these experiments increasing amounts of unlabeled protein were added to AF-labeled protein, whose concentration was held constant near its measured K_d (Table 1, Fig. 2). The resulting IC_{50} values were then converted to K_i values using the Cheng-Prussoff equation. K_i values of 3, 50, 6, and 9 nM were

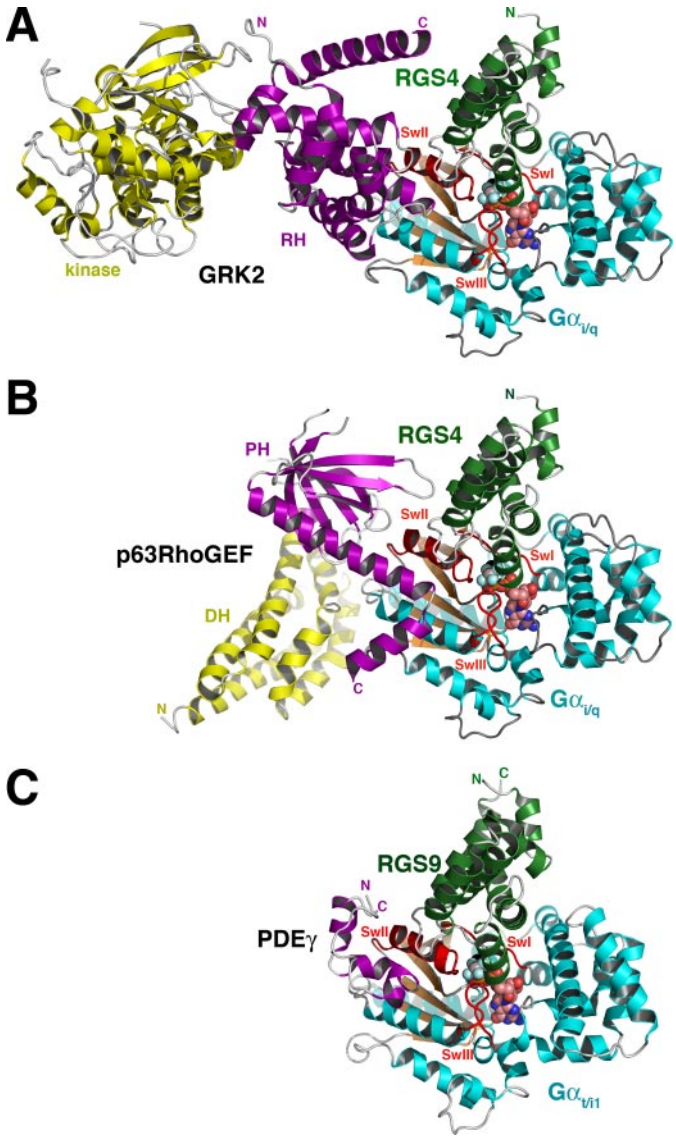

FIGURE 1. **Models of $G\alpha_q$-effector ternary complexes with RGS proteins.** To generate these models, the structure of $G\alpha_{i/q}$ in the $G\alpha_{i/q}$-GRK2-G$\beta\gamma$ complex (PDB code 2BCJ) and $G\alpha_{i/q}$ in the $G\alpha_{i/q}$-p63RhoGEF-RhoA complex (PDB code 2RGN) were superimposed on $G\alpha_i$ in the $G\alpha_i$-RGS4 structure (PDB code 1AGR), which positioned RGS4 at the RGS-binding site on the surface of $G\alpha_{i/q}$. There was no obvious steric overlap between the docked-RGS4 and either GRK2 or p63RhoGEF except for the protruding $\beta6$-$\beta7$ loop of the p63RhoGEF PH domain, which contacts the $\alpha3$ helix of the RGS box domain. However, this poorly ordered loop can likely adopt many conformations. Both the $G\alpha_q$-GRK2-G$\beta\gamma$ and $G\alpha_q$-p63RhoGEF-RhoA peripheral membrane complexes contain markers, such as the prenylation sites of Gγ and RhoA, that help define how the complexes could be oriented with respect to the cell surface. The expected membrane surface is parallel to the top of each panel. *A*, model of RGS4 bound to the $G\alpha_{i/q}$-GRK2 complex. The PH domain of GRK2 was omitted for clarity. Gα is colored *cyan* with *orange* β-strands, and the three switch regions (SwI, SwII, and SwIII) are colored *red*. Mg^{2+}·GDP·AlF_4^- in the active site of $G\alpha_{i/q}$ is shown as a sphere model. Carbons are colored *rose*, nitrogens are *blue*, oxygens are *red*, Mg^{2+} are *black*, Al^{3+} are *sand*, and F^- is *light blue*. The kinase and RGS homology domains of GRK2 are colored *yellow* and *purple*, respectively, and RGS4 is *green*. *N* and *C* denote the observed amino and carboxyl termini of the proteins. *B*, model of RGS4 bound to the $G\alpha_{i/q}$-p63RhoGEF complex. The DH and PH domains of p63RhoGEF are colored *yellow* and *purple*, respectively. *C*, structure of the RGS9-$G\alpha_{t/i1}$-PDEγ complex (PDB code 1fqj) with the Gα subunit in the same orientation as $G\alpha_{i/q}$ in *panels A* and *B*. PDEγ and RGS9 are colored *purple* and *green*, respectively.

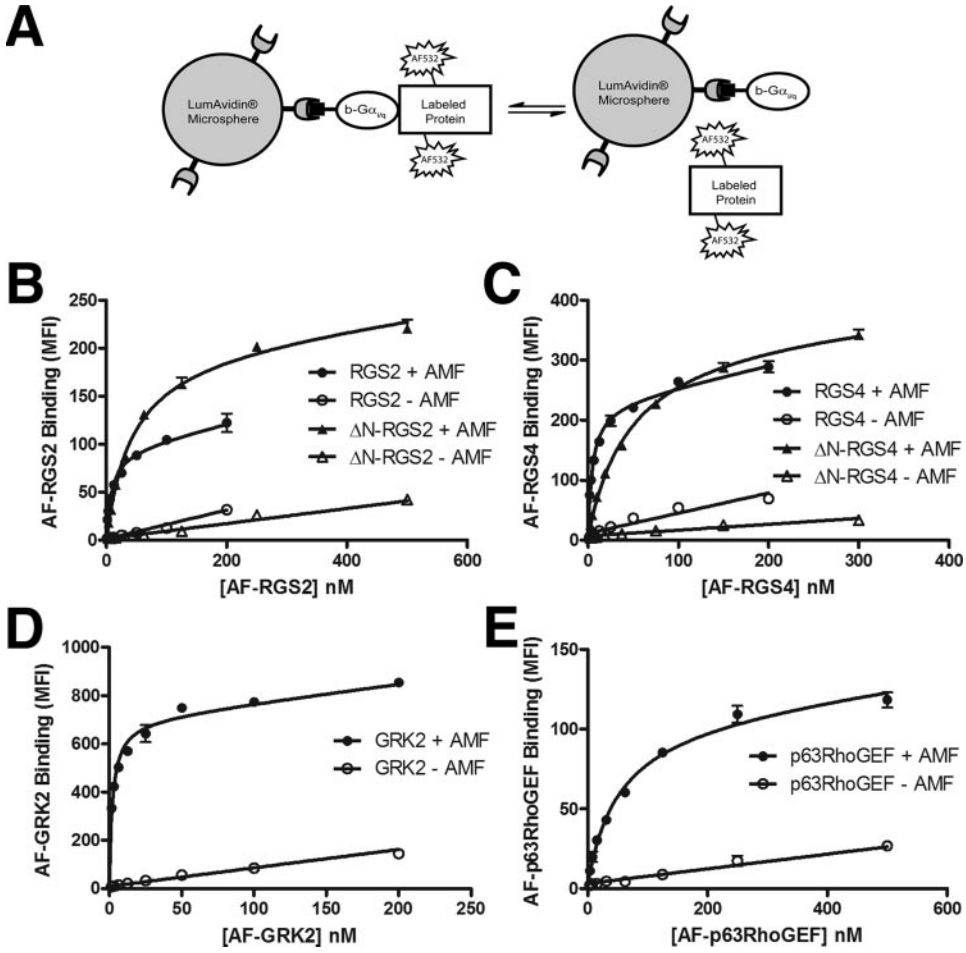

FIGURE 2. **Direct binding of fluor-labeled proteins to Gα$_{i/q}$.** *A*, scheme depicting measurement of equilibrium binding by FCPIA. Total binding was measured on a Luminex flow cytometer as the MFI of AF-labeled proteins associated with AlF_4^--activated Gα$_{i/q}$ (+*AMF*) that was biotinylated and bound to streptavidin-coated beads. Nonspecific binding was measured as the MFI from bead-bound deactivated Gα$_{i/q}$·GDP (−*AMF*). Total and nonspecific binding curves are shown for RGS2 and ΔN-RGS2 (*B*), RGS4 and ΔN-RGS4 (*C*), GRK2 (*D*), and p63RhoGEF (*E*). The data shown are representative of three or more experiments, each run in duplicate.

TABLE 1

Affinity of RGS proteins, GRK2, and p63RhoGEF for b-Gα$_{i/q}$

K_i values were determined with the Cheng-Prusoff equation using the corresponding K_d values for the AF-labeled protein.

	AF-labeled (K_d ± S.D., direct binding)	Unmodified (K_i ± S.D., competition)
RGS2	2.5 ± 1.3	6.4 ± 5.9
ΔN-RGS2	37 ± 12	
RGS4	5.3 ± 3.0	8.6 ± 4.7
ΔN-RGS4	51 ± 8.3	
GRK2	3.2 ± 1.7	3.3 ± 1.6
p63RhoGEF	83 ± 34	48 ± 14

measured for GRK2, p63RhoGEF, RGS2, and RGS4 (Table 1, Fig. 3, *B–E*, respectively).

We next used FCPIA to examine whether RGS proteins could modulate formation of the Gα$_{i/q}$-GRK2 complex. Both RGS2 and RGS4, but not inactive point mutants of RGS2 and RGS4 (N149D (60) and N128G (61), respectively), could compete with AF-GRK2 binding in the FCPIA assay (Fig. 3*B*). RGS4 could only inhibit AF-GRK2 binding to about 50%, whereas RGS2 inhibited nearly to completion. Conversely, GRK2 was not an efficacious inhibitor of the binding of either AF-RGS2 (Fig. 3*D*) or AF-RGS4 (Fig. 3*E*) to Gα$_{i/q}$ at the concentrations tested. Taken together, these data are most consistent with RGS2 and RGS4 acting as negative allosteric modulators of AF-GRK2 binding to Gα$_{i/q}$.

Next, we tested whether RGS proteins could modulate formation of the Gα$_{i/q}$-p63RhoGEF complex. As a control, we tested if GRK2 acted as an orthosteric inhibitor of AF-p63RhoGEF binding, as would be expected for two proteins that bind at the same site (Fig. 1). Indeed, GRK2 fully inhibited binding of AF-p63RhoGEF to Gα$_{i/q}$ (Fig. 3*C*). Higher concentrations of unlabeled p63RhoGEF were required for full competition, consistent with its ~10-fold higher K_d (Table 1). Both RGS2 and RGS4 could compete with AF-p63RhoGEF binding to Gα$_{i/q}$ (Fig. 3*C*), but neither could fully inhibit binding. Similar to GRK2, p63RhoGEF did not efficiently compete against AF-RGS2 and AF-RGS4 binding at the concentrations tested (Fig. 3, *D* and *E*, respectively). Thus, the data are consistent with RGS2 and RGS4 acting as negative allosteric modulators of AF-p63RhoGEF-Gα$_{i/q}$ complex formation. The allostery revealed by these competition curves does not appear to exhibit simple cooperative behavior in that GRK2 and p63RhoGEF could not inhibit AF-RGS protein binding to Gα$_{i/q}$ with the same efficacy as RGS proteins inhibit AF-GRK2/p63RhoGEF binding. However, this could simply reflect differences between AF-labeled and unlabeled proteins.

The allosteric behavior observed in the competition experiments represents only indirect proof for the formation of a ternary RGS-Gα$_{i/q}$-GRK2/p63RhoGEF complex. To use FCPIA to directly test for the formation of an RGS2/4-Gα$_{i/q}$-GRK2 complex, biotinylated RGS proteins (b-RGS2 or b-RGS4) were bound to streptavidin-coated beads and then incubated in the presence of a fixed concentration of unlabeled Gα$_{i/q}$ and increasing amounts of AF-GRK2 or AF-p63RhoGEF (Fig. 4*A*). In this experiment bead-bound fluorescence should only be observed when a ternary complex is formed, with Gα$_{i/q}$ bridging the bead-bound and AF-labeled proteins. As a control, we first showed that GRK2 has no measurable affinity for RGS proteins because in the absence of Gα$_{i/q}$, the fluorescence signal was similar to that of beads alone (data for RGS4 is shown in Fig. 4*B*). In the presence of Gα$_{i/q}$·AlF_4^-, b-RGS4 exhibited saturable binding to AF-GRK2 (Fig. 4, *B* and *C*). The measured K_d for AF-GRK2 binding to RGS4-Gα$_{i/q}$ under these conditions was ~4-fold ($n = 4$) higher than the intrinsic K_d of RGS4 for Gα$_{i/q}$.

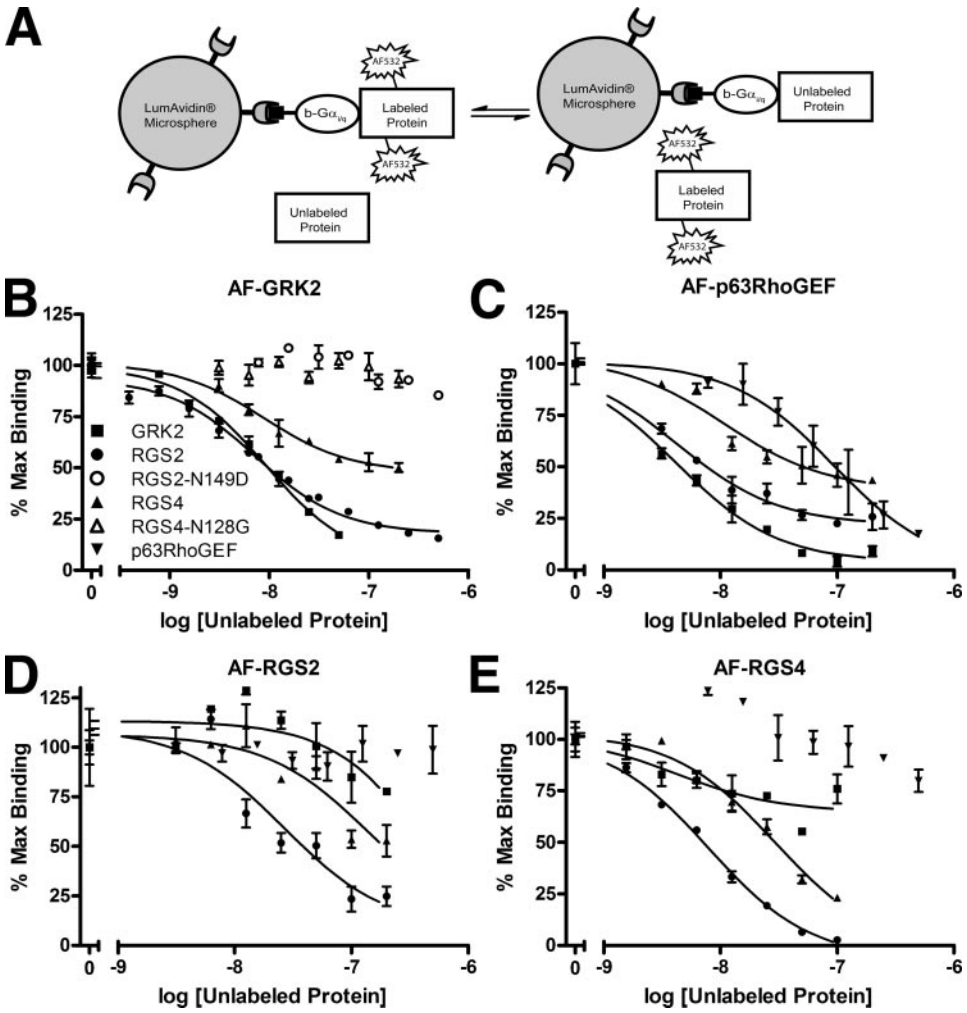

FIGURE 3. **Competition of GRK2 or p63RhoGEF with RGS proteins for b-$G\alpha_{i/q}$.** *A*, scheme depicting FCPIA competition experiments. Increasing amounts of unlabeled protein were mixed with an AF-labeled protein fixed at a concentration near its measured K_d for $G\alpha_{i/q}$. Subsequently, bead-bound b-$G\alpha_{i/q}$·AlF_4^- was added and allowed to equilibrate for at least 30 min before measurement. The data were normalized to the uninhibited maximum MFI value for each curve. The data, representative of three or more experiments run in duplicate, were fit to sigmoidal dose-response curves. *B*, competition of unlabeled GRK2, RGS2, RGS2-N149D, RGS4, and RGS4-N128G with 5 nM AF-532 GRK2 for binding to b-$G\alpha_{i/q}$·AlF_4^-. *C–E*, competition of 50 nM AF-p63RhoGEF (*C*), 10 nM AF-RGS2 (*D*), and 10 nM AF-RGS4 (*E*) with unlabeled p63RhoGEF, GRK2, RGS2, or RGS4 for binding to b-$G\alpha_{i/q}$·AlF_4^-.

This difference could be due to allosteric modulation of the GRK2-binding site on $G\alpha_{i/q}$ by RGS4. Meanwhile, RGS2 exhibited no or little ability to form an analogous ternary complex under the conditions tested (Fig. 4*C*), perhaps consistent with the fact that it exhibits stronger negative allosteric effects than RGS4 (Fig. 3*B*).

Analogous experiments with p63RhoGEF gave similar but less reproducible results, most likely because of the lower maximal signal to noise we routinely observe using AF-p63RhoGEF (*cf.* Fig. 2, *D* and *E*) and the lower affinity of p63RhoGEF for $G\alpha_{i/q}$ relative to GRK2 (Table 1). However, we could directly confirm the formation of an RGS4-$G\alpha_{i/q}$-p63RhoGEF complex by size exclusion chromatography (Fig. 4, *D* and *E*). In the experiment shown, a complex of AlF_4^--activated $G\alpha_{i/q}$ with p63RhoGEF and RGS4 was formed, and then excess GDP and Mg^{2+} was removed before the addition of apoRhoA (the presence of GDP and Mg^{2+} inhibits RhoA binding to p63RhoGEF). All four proteins eluted as a single peak from two tandem S200 gel filtration columns (Fig. 4, *D* and *E*). Because $G\alpha_{i/q}$ was limiting, peaks corresponding to free p63RhoGEF, RGS4, and RhoA were observed at lower molecular weights (Fig. 4*E*).

We had thus far observed direct ternary complexes with RGS4 but not RGS2 in our FCPIA pulldown assay and size exclusion experiments (Fig. 4). Although one might expect RGS2 and RGS4 to function similarly, in the absence of any RGS2-$G\alpha$ crystal structures it remained possible that the RGS2 and effector binding sites on $G\alpha_{i/q}$ overlap. However, we do not believe this to be the case. The N149D mutant of RGS2, equivalent to N131D point mutant in RGS16 (60) and analogous to the N128G mutant of RGS4 (61), alters a key residue that packs in the interface between RGS proteins and $G\alpha$ subunits (9). Neither RGS2-N149D nor RGS4-N128G could compete against AF-GRK2 for binding $G\alpha_{i/q}$ (Fig. 3*B*). Thus, the RGS box domains of RGS2 and RGS4 are expected to interact in the same way with the switch regions of the $G\alpha$ subunit (Fig. 1). It is true that the amino-terminal regions of these RGS proteins, which are not typically ordered in crystal structures, also have the potential to influence their behavior. In the R4 family of RGS proteins, an amphipathic helix in the amino terminus is postulated to help direct targeting of the RGS protein to membranes (58, 62–64) or to the intracellular loops of GPCRs (65) or to inhibit adenylyl cyclase (66) and the Ca^{2+} channel TRPV6 (67). In our direct binding experiments, deletion of the amino termini of RGS2 (ΔN-RGS2) and RGS4 (ΔN-RGS4) decreased affinity for $G\alpha_{i/q}$ 15- and 10-fold, respectively, compared with the full-length proteins (Fig. 2, *B* and *C*, and Table 1). Thus, the amino termini of RGS2 and RGS4 contribute to the binding affinity for $G\alpha_{i/q}$. To test the possibility that the amino terminus of RGS2, but not RGS4, docks with the effector-binding site of $G\alpha_q$ and thereby inhibits effector binding, we examined the binding of RGS2 and RGS4 to a panel of $G\alpha_q$ mutants known to be defective in effector binding (A253K, T257E, Y261N, and W263D) (36).[4] In a bead pulldown assay, all of these mutants appeared to bind RGS2 and RGS4 equally well (data not shown). Thus, we

[4] A. Shankaranarayanan, unpublished data.

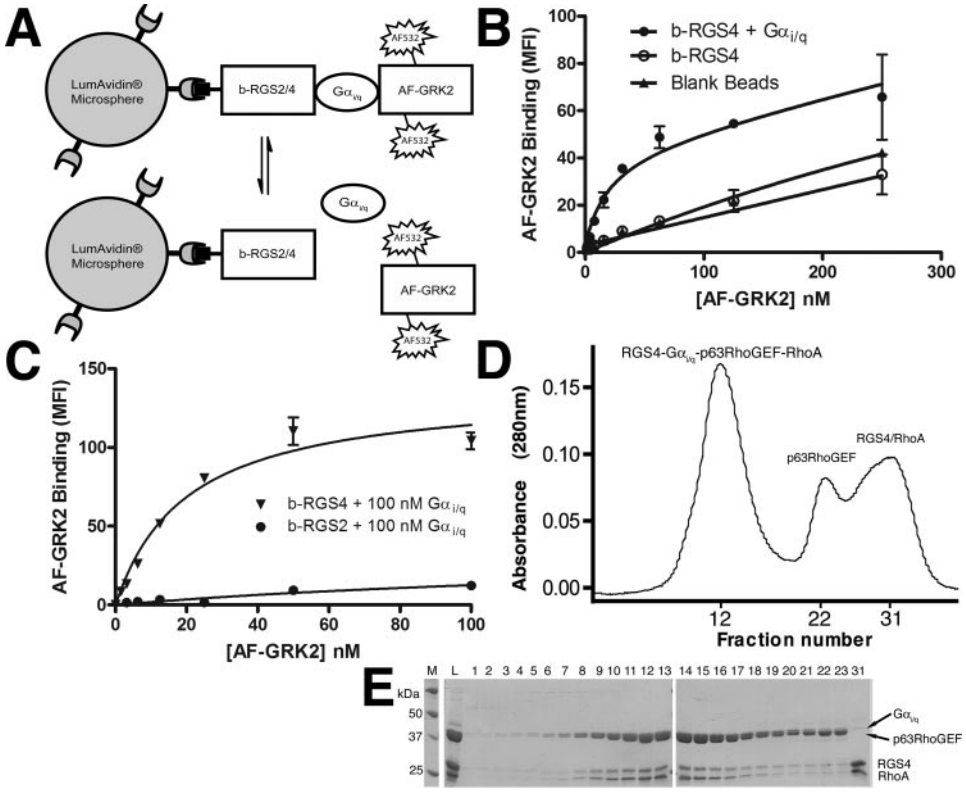

FIGURE 4. **Formation of ternary RGS complexes with Gα$_{i/q}$.** *A*, scheme depicting the direct measurement of ternary complex formation using FCPIA. *B*, AF-GRK2 does not bind to RGS4 in the absence of Gα$_{i/q}$·AlF_4^-. Shown is the total binding of AF-GRK2 to LumAvidin beads ± b-RGS4 in the presence or absence of activated Gα$_{i/q}$. The measured fluorescence of AF-GRK2 binding to beads plus b-RGS4 was similar to that of binding to beads alone. *C*, specific binding of AF-GRK2 to RGS4-Gα$_{i/q}$·AlF_4^-. In this experiment, 5 nM b-RGS2 or b-RGS4 was coupled to beads and then added to AF-GRK2 ± 100 nM Gα$_{i/q}$·AlF_4^-. RGS2 exhibited little or no affinity under these conditions. Nonspecific binding was measured as the binding of AF-GRK2 to b-RGS2/4 in the absence of Gα$_{i/q}$. Data shown are typical of four experiments, each run in duplicate. *D*, isolation of an RGS4-Gα$_{i/q}$-p63RhoGEF-RhoA quaternary complex by size exclusion chromatography. Ternary complexes of RGS4-Gα$_{i/q}$-p63RhoGEF were also purified (data not shown). *E*, peak fractions of the size exclusion run analyzed by SDS-PAGE. Proteins were visualized by Coomassie Blue stain. *M* denotes the protein standard marker lane, and *L* denotes the reaction mix load.

have no evidence that RGS2 binds in a fundamentally different way to Gα$_q$ than how RGS4 was modeled in Fig. 1. It is possible that the amino termini of RGS2 and RGS4 contribute to binding in conjunction with the RGS box through nonspecific interactions (note higher nonspecific binding for full-length RGS2 and RGS4 in Fig. 2, *B* and *C*).

To more rigorously examine the allostery mediated by RGS2 and RGS4 on Gα$_{i/q}$ complex formation, we used FCPIA to measure the binding of a fixed amount of AF-GRK2 to b-Gα$_{i/q}$·AlF_4^- in the presence of increasing concentrations of either RGS2 or RGS4 (Fig. 5, *A* and *B*). As expected for negative allosteric modulators (54), increasing amounts of RGS2 and RGS4 induced increases in the apparent K_d of AF-GRK2 that saturated at high concentrations of RGS protein. RGS2 (Fig. 5*A*) was more potent than RGS4 (Fig. 5*B*). The data were globally fit to either a simple allosteric ternary complex model (Fig. 5, *A* and *B*) or a direct competition model (supplemental Fig. S1). The curves were best fit by the allosteric model (54) with F statistics of 61 and 43 for RGS2 and RGS4, respectively, both with p values < 0.0001. The cooperativity factor (α) for RGS2 was estimated to be 22 ± 2.3 (5 separate series of curves), and that of RGS4 was estimated to be 5 ± 0.5 (2 separate series of curves). Thus, RGS2 and RGS4 appear to lower the apparent affinity of GRK2 for Gα$_{i/q}$ by up to ~22- and 5-fold, respectively. These allosteric constants were also consistent with the relative extents by which RGS2 and RGS4 inhibited binding of AF-GRK2 in competition curves (Fig. 3*B*). The extracted dissociation constants of GRK2 from the global fits were 3 ± 0.2 and 5 ± 0.5 nM for the RGS2 and RGS4 curves, respectively. The estimated dissociation constants for RGS2 and RGS4 were 10 ± 1 and 80 ± 20 nM, respectively. The GRK2 and RGS2 K_d values are similar to the dissociation constants measured by competition (Table 1) and confirm the validity of the fit for the RGS2 dose response curves. The 10-fold higher K_d calculated for RGS4 is likely a consequence of the smaller allosteric effect of RGS4 and, hence, greater inaccuracy in the global fit. Analogous experiments for AF-p63RhoGEF binding were not attempted because of its intrinsically lower signal-to-noise ratio in FCPIA measurements (Fig. 2).

Another definitive characteristic of an allosteric modulator is to change the rate of dissociation of an orthosteric ligand (68). We, therefore, used FCPIA to measure the dissociation rate of AF-GRK2 from Gα$_{i/q}$ in the presence of saturating amounts of unlabeled GRK2, GRK2+RGS2, or GRK2+RGS4 (Fig. 5*C*). RGS2 enhanced the dissociation rate of GRK2 from 0.05 to 0.17 min^{-1}, or 3.3-fold; analysis of variance $p < 0.0001$. The slight increase in the dissociation rate of GRK2 in the presence of RGS4 (0.065 min^{-1}) was not statistically significant. A 3.3-fold increase in the rate of dissociation is not enough to account for the 22-fold decrease in affinity of GRK2 for Gα$_{i/q}$ mediated by RGS2 (Fig. 5*A*). Thus, RGS2 must also decrease the rate of association of GRK2 with Gα$_{i/q}$ by ~6-fold. The significant increase in k_{off} mediated by RGS2 (Fig. 5*C*), the superior fits of our data to an allosteric model (Fig. 5, *A* and *B*, and supplemental Fig. S1), and the allosteric behavior exhibited by our competition experiments (Fig. 3) all strongly suggest that RGS2 and RGS4 are strong and weak allosteric modulators, respectively, of the effector-binding site of Gα$_q$. The fact that RGS2 ternary complexes have thus far proved more difficult to demonstrate directly may simply reflect this stronger allosteric modulation and the correspondingly greater rates that proteins dissociate from RGS2 ternary complexes.

The allostery exhibited between the RGS and effector binding sites of Gα$_{i/q}$ could also influence the activity of the proteins

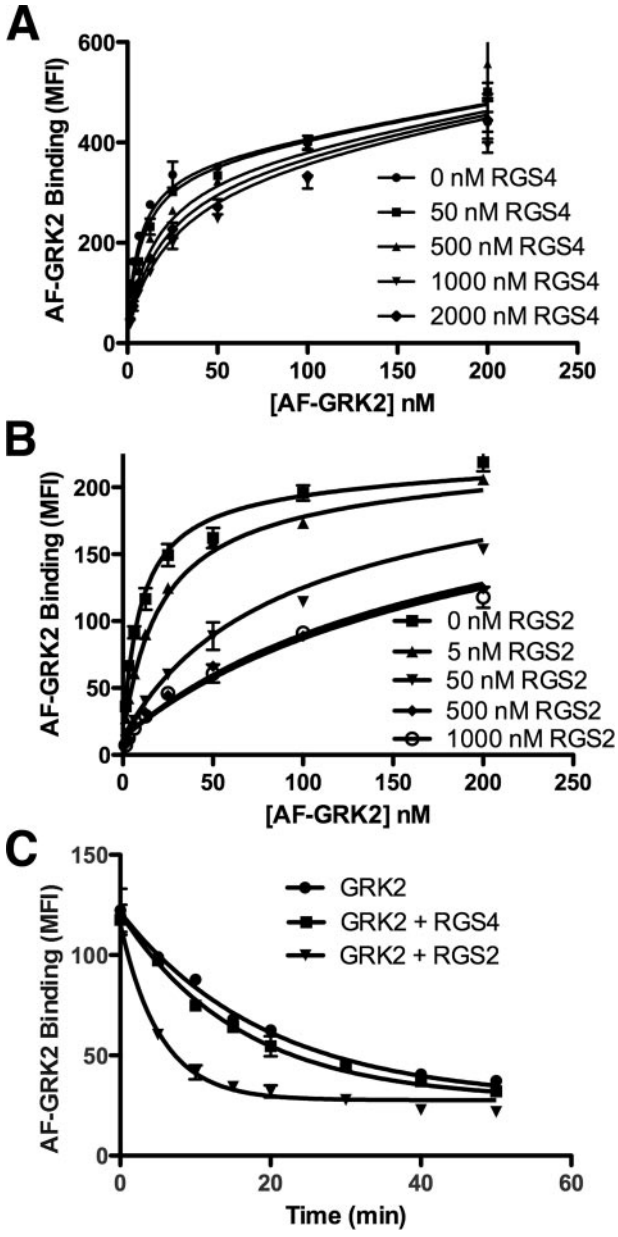

FIGURE 5. **Negative allosteric modulation between RGS proteins and GRK2 for $G\alpha_{i/q}$ binding.** *A* and *B*, dose-response curves of AF-GRK2 binding to b-$G\alpha_{i/q}$ in the presence of increasing concentrations of either RGS4 (*A*) or RGS2 (*B*). A model of negative allosteric modulation fits the data best, in part because increasing concentrations of RGS protein eventually saturate in their ability to increase the apparent K_d of AF-GRK2. The data shown are typical of 2 (RGS4) or 5 (RGS2) sets of experiments, wherein each individual curve was measured in duplicate. *C*, RGS2 modulates the intrinsic rate of GRK2 dissociation from $G\alpha_{i/q}$. The dissociation rate of AF-GRK2 (10 nM) from bead-bound b-$G\alpha_{i/q}$·AlF_4^- was measured in the presence of either 1 μM GRK2, 1 μM GRK2 plus 1 μM RGS2, or 1 μM GRK2 plus 1 μM RGS4 using FCPIA. The data shown are one of three experiments, each run with duplicate samples. RGS2 increased k_{off} of GRK2 from 0.054 ± 0.003 to 0.16 ± 0.039 min^{-1} (analysis of variance $p < 0.01$). RGS4 had a much smaller effect (0.069 ± 0.014 min^{-1}).

that bind at these sites. We first tested whether GRK2 and p63RhoGEF could modulate the GAP activity of RGS-$G\alpha_q$ complexes. GAP assays were performed using the GTPase-deficient $G\alpha_{i/q}$R183C mutant (55). Arg-183 resides at the beginning of switch I in $G\alpha_q$ and stabilizes the negative charge on the γ-phosphate of GTP during the transition state of GTP hydrolysis. The residue does not appear to interact with effectors or with RGS proteins in crystal structures. The $G\alpha_q$ R183C mutant hydrolyzes GTP slowly, facilitating measurement of GAP activity, but still activates its effectors PLCβ and p63RhoGEF and binds GRK2 (27, 69, 70). We first compared the GAP activity of 200 nM RGS2, RGS4, and ΔN-RGS2 (Fig. 6*A*). Under our experimental conditions, $G\alpha_{i/q}$R183C hydrolyzed GTP at a basal rate of 0.004 ± 0.001 min^{-1}. The addition of 200 nM RGS2 stimulated this rate 30-fold, whereas 200 nM RGS4 produced an 11-fold increase. Despite the lower apparent affinity of ΔN-RGS2 protein for b-$G\alpha_{i/q}$·AlF_4^- (Table 1), this protein had higher GAP activity than wild-type RGS2 (80-fold over basal).

To avoid saturating GAP activity, we measured GTP hydrolysis on $G\alpha_{i/q}$R183C using RGS proteins at half the prior concentration (100 nM), at which the apparent rate constants were 0.06 ± 0.02, 0.012 ± 0.001, and 0.16 ± 0.02 min^{-1} for RGS2, RGS4, and ΔN-RGS2, respectively. This also enabled us to measure the RGS-stimulated release of ^{32}P over a 15-min time course with approximately linear kinetics. In the absence of RGS proteins, neither GRK2 nor p63RhoGEF significantly stimulated GTP hydrolysis on $G\alpha_{i/q}$R183C (Fig. 6, *B* and *C*). However, at concentrations up to 50 nM, GRK2 acted synergistically with RGS4 and stimulated the rate of GTP hydrolysis up to a maximum of ~4-fold over RGS4 alone. p63RhoGEF also activated RGS4-mediated GAP activity but to a lesser extent (1.4-fold at 100 nM p63RhoGEF) (Fig. 6*C*). Point mutants of GRK2 and p63RhoGEF that are deficient in binding $G\alpha_q$ (D110A and F471E, respectively) did not enhance the rate of GTP hydrolysis by RGS4 (Fig. 6*D*), indicating that the synergistic effects of 50 nM GRK2 and p63RhoGEF are specific. The 4-fold rate enhancement we measured for RGS4 and GRK2 is similar to that observed for the cooperative interaction of RGS9 and PDEγ with $G\alpha_t$ (14, 15). Interestingly, whereas GRK2 and p63RhoGEF appeared to slightly decrease the affinity of RGS4 for $G\alpha_q$ (Fig. 3*E*), PDEγ enhanced the affinity of RGS9 for $G\alpha_t$ (16). Obviously, higher affinity for the $G\alpha_{i/q}$·AlF_4^- state is not always correlated with higher GAP activity. In contrast to RGS4, RGS2-mediated stimulation of GTP hydrolysis was not significantly affected at concentrations of either GRK2 or p63RhoGEF up to 100 nM (Fig. 6, *B* and *C*).

At the higher concentrations of GRK2 or p63RhoGEF, the GTP hydrolysis rates mediated by RGS2 and RGS4 gradually decrease. Because 400 nM GRK2-D110A and p63RhoGEF-F471E did not have this effect (supplemental Fig. S2), the slow decrease in the rate of GTP hydrolysis appears to require formation of a $G\alpha_{i/q}$-GRK2 or $G\alpha_{i/q}$-p63RhoGEF complex. Biphasic curves such as that exhibited by GRK2 and RGS4 (Fig. 6*B*) could imply multiple binding sites for GRK2 and p63RhoGEF on $G\alpha_{i/q}$, but this does not seem structurally reasonable. The decrease in GTP hydrolysis was also not dependent on the amino terminus of the RGS protein, as both ΔN-RGS2 and full-length RGS2 were inhibited at high GRK2 concentrations (Fig. 6*B*, supplemental Fig. S2). Because the GAP assay is not performed at equilibrium, it is possible that the slow decrease in the rate of GTP hydrolysis is due to a decrease in the rate of association of RGS protein at high concentrations of GRK2 or p63RhoGEF (68).

We also tested whether RGS proteins could modulate effector activity in a GAP-independent manner. Because there is no

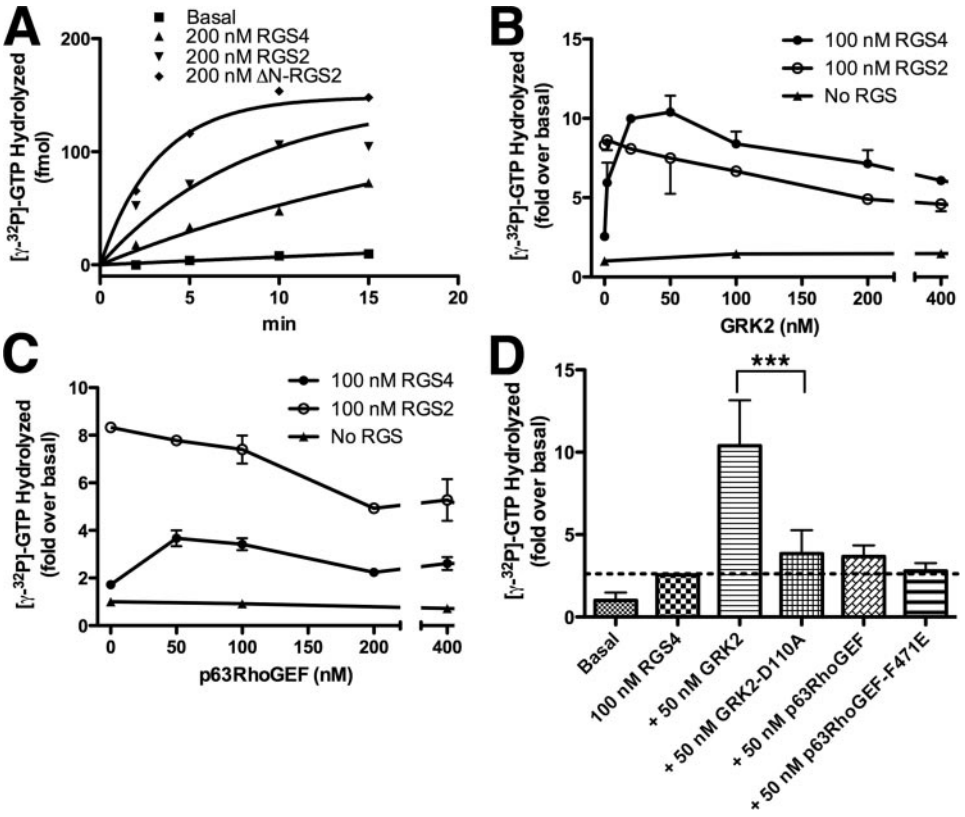

FIGURE 6. **Modulation of GAP activity by GRK2 and p63RhoGEF.** *A*, comparison of the GAP activity of 200 nM of each RGS protein on Gα$_{i/q}$R183C. In this experiment data were fit to a one-phase exponential to give rate constants of 0.005 (*Basal*), 0.12 (*RGS2*), 0.044 (*RGS4*), and 0.31 (*ΔN-RGS2*) min^{-1}. *B*, effect of GRK2 on the GTPase activity of Gα$_{i/q}$R183C·GTP in the presence or absence of 100 nM RGS protein. The amount of ^{32}P released at 2, 5, 10, and 15 min were quantified and fit to lines. The slopes were then normalized either with respect to basal activity (GRK2 alone curves) or with respect to the 100 nM RGS slope (GRK2 + RGS protein curves). The 20 nM GRK2 data point in the RGS4 curve and the 20 and 200 nM data points in the RGS2 curve are from a single experiment. The remaining data points represent the means ± S.D. of 2–7 experiments. *C*, effect of p63RhoGEF on the GTPase activity of Gα$_{i/q}$R183C·GTP in the presence or absence of 100 nM RGS proteins. The 200 nM data point in the RGS4 curve and the 50 and 200 nM data points in the RGS2 curve are from a single experiment. The remaining data points represent the means ± S.D. of 3–6 experiments. *D*, the enhancement of RGS4-stimulated GTP hydrolysis by GRK2 and p63RhoGEF is specific. The GRK2-D110A and p63RhoGEF-F471E Gα$_q$ binding-deficient mutants, used at the same concentrations as their wild-type equivalents, were deficient in stimulating GTP hydrolysis. Data shown represent the mean -fold over basal ± S.D. ($n = 3$). Data were analyzed with a Tukey post-test. *Three asterisks* indicate a significant difference between the indicated columns at the $p <$ 0.001 level.

observable increase in GRK2 activity as a function of Gα$_q$ that can be readily measured *in vitro* (70), we examined the effect of RGS2 and RGS4 on the Gα$_{i/q}$·AlF_4^--stimulated nucleotide exchange activity of p63RhoGEF. In this assay nucleotide exchange onto RhoA was measured by an increase in fluorescence polarization of a fluorescently labeled GTPγS nucleotide as it binds RhoA. Both RGS4 and RGS2 could dramatically reduce the activity of the Gα$_{i/q}$-p63RhoGEF complex (Fig. 7). The inhibition was specific, because 2 μM RGS2-N149D and 2 μM RGS4-N128G had no affect on the GEF activity. Experiments in which the addition of RGS protein was delayed by 1 or 2 h did not generate differences in inhibition (data not shown), suggesting that the observed loss of exchange activity is not a kinetic artifact due to changes in association or dissociation kinetics. Thus, it appears that RGS proteins are indeed able to modulate the activity of p63RhoGEF through both an allosteric and a GAP mechanism. These data are consistent with reports of RGS2 and RGS4 serving as effector antagonists of PLCβ (43, 49, 50). However, because PLCβ possesses its own intrinsic GAP domain (55), it is not yet clear whether the antagonism exhibited by RGS proteins against PLCβ will be allosteric or orthosteric.

DISCUSSION

Positive allosteric behavior was previously observed in the ternary complex formed by Gα$_t$, PDEγ, and RGS9. Negative allostery was exhibited between PDEγ and other RGS proteins tested, including RGS4 and RGS16 (15, 18). Our data indicate that Gα$_q$ can also form ternary complexes with RGS proteins and proteins that bind at its effector-binding site. In these complexes both RGS2 and RGS4 negatively modulate the binding of GRK2 to Gα$_{i/q}$ (Fig. 5). Competition experiments indicated that RGS2 and RGS4 also negatively modulate the binding of p63RhoGEF (Fig. 3). The allostery of these ternary complexes also had marked but disparate effects on the activity of the RGS proteins. RGS4 GAP activity on Gα$_q$ was potentiated by GRK2 and p63RhoGEF, whereas that of RGS2 was unaffected or slightly decreased (Fig. 6, *B* and *C*). In addition, we showed that the Gα$_q$-stimulated activity of p63RhoGEF was allosterically inhibited by both RGS2 and RGS4 (Fig. 7). Because Gα$_t$ is a representative member of the Gα$_i$ family and Gα$_q$ of the Gα$_{q/11}$ family, allosteric interplay between the RGS- and effector-binding sites appears possible for all Gα subunits that bind RGS proteins. The most likely conduit for such allosteric communication is the amino terminus of the helix at the beginning of switch II. This region is conformationally responsive to the nucleotide-bound state of Gα and is bracketed by interactions with both RGS protein and effector in the RGS9-Gα$_t$-PDEγ complex (Fig. 1 and Slep *et al.* (17)). This part of switch II also contributes a critical glutamine residue to the hydrolytic site of Gα (12). Thus, subtle changes in the conformation of this region could have profound effects on the affinity of effectors and GAPs and on the rate of GTP hydrolysis.

Despite the great structural diversity exhibited by the protein domains that interact with the effector-binding sites of Gα$_q$ and Gα$_{i/t}$ (Fig. 1), the ability to form ternary complexes between effectors, Gα subunits, and RGS proteins appears remarkably well conserved. What physiological roles might these ternary complexes serve? Segregation of the effector and RGS binding sites on the Gα subunit enables RGS proteins to modulate sig-

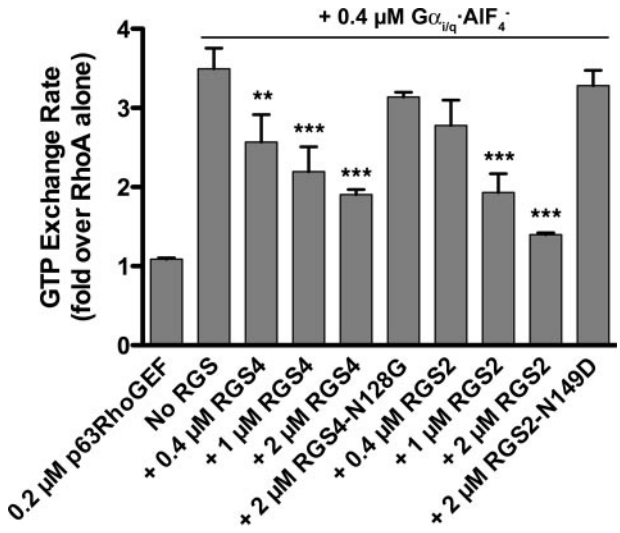

FIGURE 7. **Inhibition of Gα$_{i/q}$-stimulated p63RhoGEF activity by RGS2 and RGS4.** Nucleotide exchange on RhoA was monitored by the increase in fluorescence millipolarization of BODIPY FL GTPγS upon binding RhoA. The resulting data were fit as one phase exponentials and are expressed here as the average -fold over basal exchange ± S.D. from three independent experiments, each measured in triplicate. *Two asterisks* indicate an analysis of variance $p < 0.01$, and *three asterisks* indicate an analysis of variance $p < 0.001$ between the indicated column and the nucleotide exchange rate of the *No RGS* column.

nal transduction of effector-bound Gα subunits. This may enable faster rates of signal termination because RGS proteins would not have to compete for the same site as effectors. The enhancement of the GAP activity of RGS9 on Gα$_t$ mediated by PDEγ is required for physiological rates of signal termination in rod cells. Because of this requirement, the synergy between PDEγ and RGS9 has been proposed to be a mechanism that helps to ensure that phototransduction occurs through PDE before GAP activity is brought to bear, preventing a potential short circuit (18, 71). Thus, Gα$_t$, PDEγ and RGS9 collaborate to achieve both efficient signal transduction (no short circuit) and high time resolution (rapid GTP hydrolysis on Gα$_t$) (72). Gα$_q$ is the Gα subunit responsible for invertebrate phototransduction and from an evolutionary perspective may have similar requirements for efficient effector coupling and rapid signal termination. Invertebrate phototransduction is mediated by a phospholipase C enzyme, which like vertebrate PLCβs, has its own intrinsic GAP domain (73). Indeed, vertebrate PLCβ1 can stimulate GTP hydrolysis on Gα$_q$ by 3 orders of magnitude (8) to rates similar to the rate of signal termination in invertebrate vision (74). The presence of both a GAP and effector in the same molecule is thought to ensure both efficient signal transduction and high time resolution. However, like PDEγ, GRK2 and p63RhoGEF have little or no GAP activity for Gα$_q$ in the absence of RGS proteins. When challenged by RGS4, which can accelerate GTP hydrolysis on Gα$_q$ at even higher rates than PLCβ1 (8), a mechanism to avoid a short circuit may become necessary. The enhanced GAP activity exhibited by RGS4 in the presence of GRK2/p63RhoGEF could, therefore, represent a way to keep the rates of Gα$_q$ GTP hydrolysis lower until an effector is already engaged with Gα$_q$. The fact that RGS proteins can allosterically affect p63RhoGEF activity (Fig. 7) represents additional evidence that RGS proteins can serve a role in tuning rather than simply squelching G$_q$ signal transduction. In fact, if Gα$_q$ is indeed rapidly cycled by GPCRs (12, 40), then tuning the amplitude of the signal may be the ultimate manifestation of RGS activity on Gα$_q$ in cells.

RGS2 exhibits GAP activity that is not positively cooperative with effector binding (Fig. 6) and has a much stronger negative allosteric effect than RGS4 on the affinity of proteins that bind at the effector site of Gα$_q$ (Figs. 3 and 5). Clearly, two different RGS proteins, even members of the same RGS subfamily, can have strikingly different allosteric effects. The ability to form distinct complexes between Gα$_q$, effectors and RGS proteins with different allosteric properties may ultimately allow for a greater ability to tune the strength and duration of signal transduction in a manner that meets the specific requirements of a particular cell-type or physiological setting. For example, RGS2 may be up-regulated by cells in situations when a short circuit of Gα$_q$ signaling would be beneficial.

GRK2 and p63RhoGEF are similar not only in the manner in which they bind Gα$_q$ (Fig. 1) but also in the way they are allosterically regulated by RGS proteins. Our data, therefore, support the idea that GRK2 is a *bona fide* effector target of Gα$_q$ whose activity can, therefore, be modulated by the action of RGS proteins *in vivo*. Because Gα$_q$ as of yet has no obvious effect on the catalytic activity of GRK2 *in vitro* (70), the role of Gα$_q$ in regulating GRK2 signaling might simply be translocation of the soluble enzyme to the vicinity of its targets. Although recruitment of the RGS homology domain of GRK2 to the membrane by activated Gα$_q$ has been observed in cells (35, 75), membrane translocation of GRK2 has historically been attributed to Gβγ subunits (76, 77). Under conditions near physiological ionic strength, GRK2 binds to Gα$_{i/q}$·AlF$_4^-$ with >10-fold higher affinity than to Gβγ subunits in detergent micelles.[5] Gα$_q$ might, therefore, be the principal route by which GRK2 is recruited to membranes when Gα$_q$-coupled receptors are activated, especially if Gβγ were involved in interactions with other peripheral membrane proteins (*e.g.* PLCβ). However, even if Gβγ were solely responsible for the membrane translocation of GRK2, RGS-Gα$_q$ complexes could still modulate GRK2 activity by controlling how long Gβγ interacts with GRK2. RGS-accelerated GTP hydrolysis, allosterically tuned by GRK2, would more rapidly return Gα$_q$ to its deactivated GDP-bound state, which would then sequester Gβγ from GRK2.

The best-established "downstream" target of GRK2 is of course an activated GPCR. Phosphorylation of these GPCRs recruits arrestin, uncouples G proteins from the receptor, targets the receptor for clathrin-mediated endocytosis, and activates arrestin-mediated pathways. The idea that RGS proteins might also regulate this activity is an intriguing one and suggests that conditions that lead to up-regulation of RGS proteins might also lead to a loss of GRK2 and GRK3-mediated phosphorylation of at least Gα$_q$-coupled GPCRs.

In summary, our data support the idea that RGS proteins are the third component of a ternary complex formed by Gα$_i$ and Gα$_q$ subunits during active signal transduction. Because GPCRs are also reported to interact with RGS proteins, an acti-

[5] V. Tesmer, unpublished data.

vated receptor may be a fourth obligate member of this complex. Not only has nature mandated that structurally diverse effectors and RGS proteins co-exist in complexes with $G\alpha_q$, but it also appears that $G\alpha_q$ subunits have evolved to adopt a specific orientation at the membrane while engaging effectors (Fig. 1). This orientation may be conserved for the purpose of promoting productive interaction with membrane- or receptor-associated RGS proteins and may also provide the underlying molecular basis for the rapid nucleotide cycling of $G\alpha$ subunits that occurs in the presence of RGS proteins at activated G_q-coupled receptors (12, 40).

Acknowledgments—We thank T. Kawano and N. Hajicek (University of Illinois College of Medicine, Chicago) for help with $G\alpha_q$ GTPase assays and C. Coco (Life Sciences Institute, University of Michigan) for technical assistance.

REFERENCES

1. Gilman, A. G. (1987) *Annu. Rev. Biochem.* **56,** 615–649
2. Neves, S. R., Ram, P. T., and Iyengar, R. (2002) *Science* **296,** 1636–1639
3. Berstein, G., Blank, J. L., Jhon, D. Y., Exton, J. H., Rhee, S. G., and Ross, E. M. (1992) *Cell* **70,** 411–418
4. Kozasa, T., Jiang, X., Hart, M. J., Sternweis, P. M., Singer, W. D., Gilman, A. G., Bollag, G., and Sternweis, P. C. (1998) *Science* **280,** 2109–2111
5. Berman, D. M., Wilkie, T. M., and Gilman, A. G. (1996) *Cell* **86,** 445–452
6. Watson, N., Linder, M. E., Druey, K. M., Kehrl, J. H., and Blumer, K. J. (1996) *Nature* **383,** 172–175
7. Zhong, H., Wade, S. M., Woolf, P. J., Linderman, J. J., Traynor, J. R., and Neubig, R. R. (2003) *J. Biol. Chem.* **278,** 7278–7284
8. Mukhopadhyay, S., and Ross, E. M. (1999) *Proc. Natl. Acad. Sci. U. S. A.* **96,** 9539–9544
9. Tesmer, J. J. G., Berman, D. M., Gilman, A. G., and Sprang, S. R. (1997) *Cell* **89,** 251–261
10. Tesmer, J., Sunahara, R., Gilman, A., and Sprang, S. (1997) *Science* **278,** 1907–1916
11. Sunahara, R. K., Tesmer, J. J. G., Gilman, A. G., and Sprang, S. R. (1997) *Science* **278,** 1943–1947
12. Sprang, S. R., Chen, Z., and Du, X. (2007) *Adv. Protein Chem.* **74,** 1–65
13. Arshavsky, V., and Bownds, M. D. (1992) *Nature* **357,** 416–417
14. He, W., Cowan, C. W., and Wensel, T. G. (1998) *Neuron* **20,** 95–102
15. McEntaffer, R. L., Natochin, M., and Artemyev, N. O. (1999) *Biochemistry* **38,** 4931–4937
16. Skiba, N. P., Yang, C. S., Huang, T., Bae, H., and Hamm, H. E. (1999) *J. Biol. Chem.* **274,** 8770–8778
17. Slep, K. C., Kercher, M. A., He, W., Cowan, C. W., Wensel, T. G., and Sigler, P. B. (2001) *Nature* **409,** 1071–1077
18. Nekrasova, E., Berman, D., Rustandi, R., Hamm, H., Gilman, A., and Arshavsky, V. (1997) *Biochemistry* **36,** 7638–7643
19. Natochin, M., Granovsky, A. E., and Artemyev, N. O. (1997) *J. Biol. Chem.* **272,** 17444–17449
20. Wieland, T., Chen, C. K., and Simon, M. I. (1997) *J. Biol. Chem.* **272,** 8853–8856
21. Offermanns, S., and Simon, M. I. (1998) *Oncogene* **17,** 1375–1381
22. Hubbard, K. B., and Hepler, J. R. (2006) *Cell. Signal.* **18,** 135–150
23. Dorn, G. W., Jr., and Force, T. (2005) *J. Clin. Investig.* **115,** 527–537
24. Harris, D. M., Cohn, H. I., Pesant, S., Zhou, R. H., and Eckhart, A. D. (2007) *Am. J. Physiol. Heart Circ. Physiol.* **293,** 3072–3079
25. Rhee, S. G. (2001) *Annu. Rev. Biochem.* **70,** 281–312
26. Lutz, S., Freichel-Blomquist, A., Yang, Y., Rumenapp, U., Jakobs, K. H., Schmidt, M., and Wieland, T. (2005) *J. Biol. Chem.* **280,** 11134–11139
27. Lutz, S., Shankaranarayanan, A., Coco, C., Ridilla, M., Nance, M. R., Vettel, C., Baltus, D., Evelyn, C. R., Neubig, R. R., Wieland, T., and Tesmer, J. J. (2007) *Science* **318,** 1923–1927
28. Williams, S. L., Lutz, S., Charlie, N. K., Vettel, C., Ailion, M., Coco, C., Tesmer, J. J., Jorgensen, E. M., Wieland, T., and Miller, K. G. (2007) *Genes Dev.* **21,** 2731–2746
29. Rojas, R. J., Yohe, M. E., Gershburg, S., Kawano, T., Kozasa, T., and Sondek, J. (2007) *J. Biol. Chem.* **282,** 29201–29210
30. Theilade, J., Haunso, S., and Sheikh, S. P. (2001) *Curr. Drug Targets Immune Endocr. Metabol. Dis.* **1,** 139–151
31. Pitcher, J. A., Freedman, N. J., and Lefkowitz, R. J. (1998) *Annu. Rev. Biochem.* **67,** 653–692
32. Willets, J. M., Nahorski, S. R., and Challiss, R. A. (2005) *J. Biol. Chem.* **280,** 18950–18958
33. Willets, J. M., Nash, M. S., Challiss, R. A., and Nahorski, S. R. (2004) *J. Neurosci.* **24,** 4157–4162
34. Iwata, K., Luo, J., Penn, R. B., and Benovic, J. L. (2005) *J. Biol. Chem.* **280,** 2197–2204
35. Sterne-Marr, R., Tesmer, J. J., Day, P. W., Stracquatanio, R. P., Cilente, J. A., O'Connor, K. E., Pronin, A. N., Benovic, J. L., and Wedegaertner, P. B. (2003) *J. Biol. Chem.* **278,** 6050–6058
36. Tesmer, V. M., Kawano, T., Shankaranarayanan, A., Kozasa, T., and Tesmer, J. J. (2005) *Science* **310,** 1686–1690
37. Usui, I., Imamura, T., Babendure, J. L., Satoh, H., Lu, J. C., Hupfeld, C. J., and Olefsky, J. M. (2005) *Mol. Endocrinol.* **19,** 2760–2768
38. Peregrin, S., Jurado-Pueyo, M., Campos, P. M., Sanz-Moreno, V., Ruiz-Gomez, A., Crespo, P., Mayor, F., Jr., and Murga, C. (2006) *Curr. Biol.* **16,** 2042–2047
39. Cant, S. H., and Pitcher, J. A. (2005) *Mol. Biol. Cell* **16,** 3088–3099
40. Ross, E. M., and Wilkie, T. M. (2000) *Annu. Rev. Biochem.* **69,** 795–827
41. Bansal, G., Druey, K. M., and Xie, Z. (2007) *Pharmacol. Ther.* **116,** 473–495
42. Xu, X., Zeng, W., Popov, S., Berman, D. M., Davignon, I., Yu, K., Yowe, D., Offermanns, S., Muallem, S., and Wilkie, T. M. (1999) *J. Biol. Chem.* **274,** 3549–3556
43. Heximer, S. P., Watson, N., Linder, M. E., Blumer, K. J., and Hepler, J. R. (1997) *Proc. Natl. Acad. Sci. U. S. A.* **94,** 14389–14393
44. Ingi, T., Krumins, A. M., Chidiac, P., Brothers, G. M., Chung, S., Snow, B. E., Barnes, C. A., Lanahan, A. A., Siderovski, D. P., Ross, E. M., Gilman, A. G., and Worley, P. F. (1998) *J. Neurosci.* **18,** 7178–7188
45. Heximer, S. P., Srinivasa, S. P., Bernstein, L. S., Bernard, J. L., Linder, M. E., Hepler, J. R., and Blumer, K. J. (1999) *J. Biol. Chem.* **274,** 34253–34259
46. Scheschonka, A., Dessauer, C. W., Sinnarajah, S., Chidiac, P., Shi, C. S., and Kehrl, J. H. (2000) *Mol. Pharmacol.* **58,** 719–728
47. Hao, J., Michalek, C., Zhang, W., Zhu, M., Xu, X., and Mende, U. (2006) *J. Mol. Cell. Cardiol.* **41,** 51–61
48. Karakoula, A., Tovey, S. C., Brighton, P. J., and Willars, G. B. (2008) *Eur. J. Pharmacol.* **587,** 16–24
49. Hepler, J. R., Berman, D. M., Gilman, A. G., and Kozasa, T. (1997) *Proc. Natl. Acad. Sci. U. S. A.* **94,** 428–432
50. Anger, T., Zhang, W., and Mende, U. (2004) *J. Biol. Chem.* **279,** 3906–3915
51. Kristelly, R., Earnest, B. T., Krishnamoorthy, L., and Tesmer, J. J. (2003) *Acta Crystallogr. D Biol. Crystallogr.* **59,** 1859–1862
52. Heximer, S. P. (2004) *Methods Enzymol.* **390,** 65–82
53. Lodowski, D. T., Barnhill, J. F., Pitcher, J. A., Capel, W. D., Lefkowitz, R. J., and Tesmer, J. J. (2003) *Acta Crystallogr. D Biol. Crystallogr.* **59,** 936–939
54. Ehlert, F. J. (1988) *Mol. Pharmacol.* **33,** 187–194
55. Chidiac, P., and Ross, E. M. (1999) *J. Biol. Chem.* **274,** 19639–19643
56. Soundararajan, M., Willard, F. S., Kimple, A. J., Turnbull, A. P., Ball, L. J., Schoch, G. A., Gileadi, C., Fedorov, O. Y., Dowler, E. F., Higman, V. A., Hutsell, S. Q., Sundstrom, M., Doyle, D. A., and Siderovski, D. P. (2008) *Proc. Natl. Acad. Sci. U. S. A.* **105,** 6457–6462
57. Roman, D. L., Talbot, J. N., Roof, R. A., Sunahara, R. K., Traynor, J. R., and Neubig, R. R. (2007) *Mol. Pharmacol.* **71,** 169–175
58. Gu, S., He, J., Ho, W. T., Ramineni, S., Thal, D. M., Natesh, R., Tesmer, J. J., Hepler, J. R., and Heximer, S. P. (2007) *J. Biol. Chem.* **282,** 33064–33075
59. Kreutz, B., Yao, D. M., Nance, M., Tanabe, S., Tesmer, J. J. G., and Kozasa, T. (2006) *Biochemistry* **45,** 167–174
60. Natochin, M., McEntaffer, R. L., and Artemyev, N. O. (1998) *J. Biol. Chem.* **273,** 6731–6735

61. Posner, B. A., Mukhopadhyay, S., Tesmer, J. J., Gilman, A. G., and Ross, E. M. (1999) *Biochemistry* **38,** 7773–7779
62. Zeng, W., Xu, X., Popov, S., Mukhopadhyay, S., Chidiac, P., Swistok, J., Danho, W., Yagaloff, K. A., Fisher, S. L., Ross, E. M., Muallem, S., and Wilkie, T. M. (1998) *J. Biol. Chem.* **273,** 34687–34690
63. Chen, C., Seow, K. T., Guo, K., Yaw, L. P., and Lin, S. C. (1999) *J. Biol. Chem.* **274,** 19799–19806
64. Bernstein, L. S., Grillo, A. A., Loranger, S. S., and Linder, M. E. (2000) *J. Biol. Chem.* **275,** 18520–18526
65. Bernstein, L. S., Ramineni, S., Hague, C., Cladman, W., Chidiac, P., Levey, A. I., and Hepler, J. R. (2004) *J. Biol. Chem.* **279,** 21248–21256
66. Salim, S., Sinnarajah, S., Kehrl, J. H., and Dessauer, C. W. (2003) *J. Biol. Chem.* **278,** 15842–15849
67. Schoeber, J. P., Topala, C. N., Wang, X., Diepens, R. J., Lambers, T. T., Hoenderop, J. G., and Bindels, R. J. (2006) *J. Biol. Chem.* **281,** 29669–29674
68. Christopoulos, A., and Kenakin, T. (2002) *Pharmacol. Rev.* **54,** 323–374
69. Conklin, B. R., Chabre, O., Wong, Y. H., Federman, A. D., and Bourne, H. R. (1992) *J. Biol. Chem.* **267,** 31–34
70. Carman, C. V., Parent, J. L., Day, P. W., Pronin, A. N., Sternweis, P. M., Wedegaertner, P. B., Gilman, A. G., Benovic, J. L., and Kozasa, T. (1999) *J. Biol. Chem.* **274,** 34483–34492
71. Arshavsky, V. Y., and Pugh, E. N., Jr. (1998) *Neuron* **20,** 11–14
72. Arshavsky, V. Y., Lamb, T. D., and Pugh, E. N., Jr. (2002) *Annu. Rev. Physiol.* **64,** 153–187
73. Cook, B., Bar-Yaacov, M., Cohen Ben-Ami, H., Goldstein, R. E., Paroush, Z., Selinger, Z., and Minke, B. (2000) *Nat. Cell Biol.* **2,** 296–301
74. Ranganathan, R., Harris, G. L., Stevens, C. F., and Zuker, C. S. (1991) *Nature* **354,** 230–232
75. Day, P. W., Carman, C. V., Sterne-Marr, R., Benovic, J. L., and Wedegaertner, P. B. (2003) *Biochemistry* **42,** 9176–9184
76. Koch, W. J., Hawes, B. E., Inglese, J., Luttrell, L. M., and Lefkowitz, R. J. (1994) *J. Biol. Chem.* **269,** 6193–6197
77. Koch, W. J., Rockman, H. A., Samama, P., Hamilton, R. A., Bond, R. A., Milano, C. A., and Lefkowitz, R. J. (1995) *Science* **268,** 1350–1353